J. Geomag. Geoelectr., **40**, 1221-1233, 1988

Pulsed Electron Beam Emission in Space

T. NEUBERT[1], J. G. HAWKINS[1], G. D. REEVES[1], P. M. BANKS[1], R. I. BUSH[1], P. R. WILLIAMSON[1], D. A. GURNETT[2], and W. J. RAITT[3]

[1]*STARLAB, Stanford University, Stanford, CA 94305, U.S.A.*
[2]*Department of Physics and Astronomy, University of Iowa, Iowa City, Iowa 52242, U.S.A.*
[3]*Center for Atmospheric and Space Sciences, Utah State University, Logan, Utah 84322, U.S.A.*

(Received February 22, 1988; Accepted June 3, 1988)

During the Spacelab-2 mission of July, 1985, electron beams (1 keV, 50-150 mA) pulsed at ELF and VLF frequencies were emitted from the Space Shuttle Orbiter. The wave fields generated by the beam were monitored by a Plasma Diagnostics Package (PDP), which was released as a free-flying sub-satellite during a six hour period. Measurements of the Orbiter potential and the return current during beam emissions were obtained from a Charge and Current Probe (CCP) mounted in the payload bay. Results from the PDP and CCP are presented.

1. Introduction

Some effort in recent years has gone into the study of the radiation generated by pulsed electron beams emitted from space platforms (HOLZWORTH and KOONS, 1981; WINCKLER *et al.*, 1985; BUSH *et al.*, 1987; REEVES *et al.*, 1988a). The background for this interest is partly the idea that pulsed beams may replace conventional antennas in space for certain communication purposes. An issue which must be addressed when considering this option is the charging of the space platform during beam emissions and the formation of a region of enhanced negative space charge close to the beam nozzle. These effects are important to understand because they may limit the amount of beam current escaping the platform and distort the beam coherence. In the Space Experiments with Particle Accelerators (SEPAC) flown on the Spacelab-1 Shuttle mission, for instance, it was found that when the main thruster engine bells were in the wake (they constitute the largest conducting area of the Orbiter), the Orbiter may have charged to the beam potential of 5 keV when the beam current exceeded 100 mA, thereby partly inhibiting the beam from escaping the Orbiter (SASAKI *et al.*, 1986). However, this conclusion is somewhat controversial. High Orbiter charging effects during electron beam emissions are not supported by observations from the 1ES019A spectrometer also flown on the SEPAC Shuttle mission (WATERMANN *et al.*, 1988).

Recent numerical simulations show that when the electron beam density exceeds the ambient plasma density, a negative space charge may build up in a region close to the beam nozzle. This will reflect a portion of the beam electrons and greatly distort the escaping portions of the beam (PRITCHETT and WINGLEE, 1987).

The questions of spacecraft charging and loss of beam coherence are addressed in the paper by means of observations made during the Spacelab-2 mission of the Space Shuttle Orbiter. The observations include Orbiter charging and return currents during electron beam emissions and wave fields generated by pulsed and continuous beams.

Spacelab-2 was launched into an almost circular orbit with a nominal altitude of 325 km and an inclination of 49.5°. A Fast Pulse Electron Generator (FPEG) was mounted on the port side of the Orbiter. The beam energy was 1 keV and the beam current could be set to 50, 100, or 150 mA by selecting a combination of two separate electron sources. The beam could be emitted in a continuous mode (DC) or in a pulsed mode (AC), where the beam current was almost perfectly square-wave modulated with a nominal pulse rise time of 10^{-7} s.

A Charge and Current Probe (CCP) was mounted on the starboard side of the payload bay. The Charge Probe has a conducting surface covered by a dielectric layer, and it measures changes in the potential induced across the dielectric layer. The Current Probe measures the current flowing through a gold plated surface and is mounted next to the Charge Probe. The FPEG and the CCP were part of the Vehicle Charging and Potential experiment (VCAP), which was also flown on STS-3/OSS-1. It is described in more detail in BANKS *et al.* (1987).

A Plasma Diagnostics Package (PDP) was stored in the payload bay. During a six hour period the PDP was released as a free-flying satellite to co-orbit at distances up to 300 m from the Shuttle. The PDP carried an array of plasma diagnostics equipment, including an electric dipole antenna and a magnetic search coil. The antennas were connected alternately for 52.2 s to the wide-band wave receiver. The receiver scanned a 30 kHz frequency range by selecting 10 kHz bands in the following order: 0–10 kHz (25.6 s), 20–10 kHz (12.8 s), and 20–30 kHz (12.8 s). The receiver output was controlled by an Automatic Gain Control system (AGC), which ensured a 100 dB dynamic range and a roughly constant output level. The output was telemetered in analog form and was later digitized at 25 kHz. In addition, the antennas were connected to a number of filterbank receivers with a coverage in frequency from 31 Hz to 800 MHz. For a description of the PDP instruments, see SHAWHAN *et al.* (1984).

2. Observations

2.1 *Orbiter charging and return currents*

We have attempted to correlate the measurements of the CCP during DC electron beam emissions with the ambient ionospheric densities. This imposes a problem since the interactions between the Shuttle Orbiter and the ionosphere frequently prevent accurate measurements of ambient plasma parameters from the payload bay (SISKIND *et al.*, 1983; RAITT *et al.*, 1984; GREBOWSKY *et al.*, 1987).

During the Spacelab-2 mission, the only in situ measurements of the plasma density away from the plasma perturbations associated with the Orbiter were performed during a 6 hour period when the PDP became a free-flying satellite. For other times of the mission, we must rely on values of the ambient density predicted by the International Reference Ionosphere (IRI) model (BILITZA, 1986). The accuracy of the IRI model has been assessed by comparing its predictions with the measurements from a Langmuir probe on the PDP during the 6 hour free-flight. It was found that the predicted values of the density were, in general, higher than the measured ones, at times up to an order of magnitude higher, but that the general trend of day/night variations etc. was captured well by the model. Much of this difference can be attributed to the fact that the PDP measurements were made during a period of general magnetospheric disturbance with $K_p=5^+$ at the time of the PDP release. Deep electron density troughs were seen at high magnetic latitudes, while the plasma density at the geomagnetic equator dropped below 10^3 cm^{-3}. These features tended to become less visible as time went on in the PDP free-flight period.

With this caution in mind, results from the Charge Probe are shown in Fig. 1 as function of ambient plasma density as predicted by the IRI model. The figure shows a summary of the Charge Probe measurements during all DC beam emissions performed during the Spacelab-2 mission (HAWKINS, 1988). For high ambient plasma densities the charging level of the Orbiter is low, while for low densities the Orbiter charges to high levels. The charge probe does not give absolute measurements of the Orbiter potential, but rather a measurement of the potential drop across a dielectric surface covering the probe. For low charging levels and thin potential sheaths, the probe measurement is close to the vehicle potential, while for higher potential levels and extended sheath regions, the probe generally measures a potential which is lower than the vehicle potential.

A threshold in the ambient plasma density for which the Orbiter charges to high levels can be estimated from Fig. 1. This is about 3×10^5 cm^{-3} for 100 mA beam current and 1.5×10^5 cm^{-3} for 50 mA current. If we consider the threshold density to be the density at which the thermal electron current from the ionosphere balances the beam current, then we find the effective current collecting area of the Orbiter to be about 42 m^2 for an electron temperature of 1000 K (HAWKINS, 1988). This area is comparable to, but somewhat larger than, the area of the main engine bells which have a surface area of about 30 m^2. They constitute the largest, but not all, the current collecting area of the Orbiter. We thus interpret the threshold seen in the charging level as the ambient plasma density level at which the electron thermal current equals the beam current. At lower densities the Orbiter has to charge to high potentials in order to draw a sufficient return current.

Figure 2 shows Current Probe measurements during DC beam emissions as function of ambient plasma density predicted by the IRI model. Also shown is the electron thermal current that can be drawn to the probe for temperatures of 1000 K and 3000 K. Data show that the current to the probe depends on the Orbiter attitude. This is an ion wake phenomena, since the Orbiter velocity, V_s, is about 7.8 km/s, which is much larger than the ion thermal velocity (about 1 km/s). Thus the current to the probe varies greatly from ram to wake conditions (RAITT *et al.*, 1984; GREBOWSKY *et al.*, 1987). Furthermore, the probe potential is shifted by the $(\boldsymbol{V}_s\times\boldsymbol{B})\cdot\boldsymbol{L}$ induced potential, where $\boldsymbol{L}$ is a vector pointing from the engine bells to the

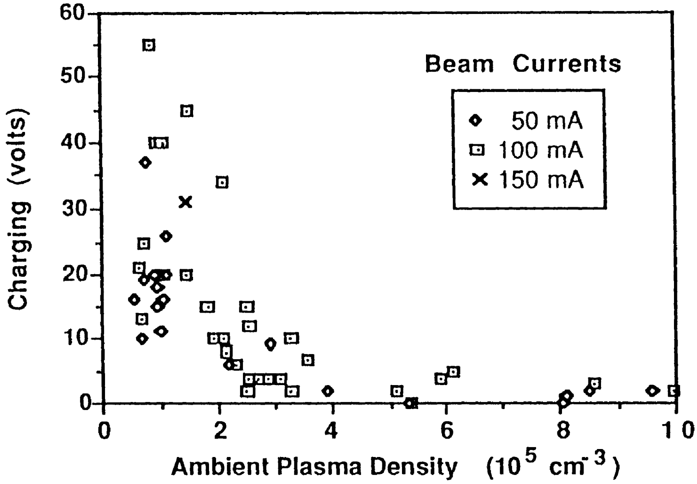

Fig. 1. Vehicle charging during DC electron beam emissions measured by the CCP charge probe as function of ambient plasma density estimated from the IRI model.

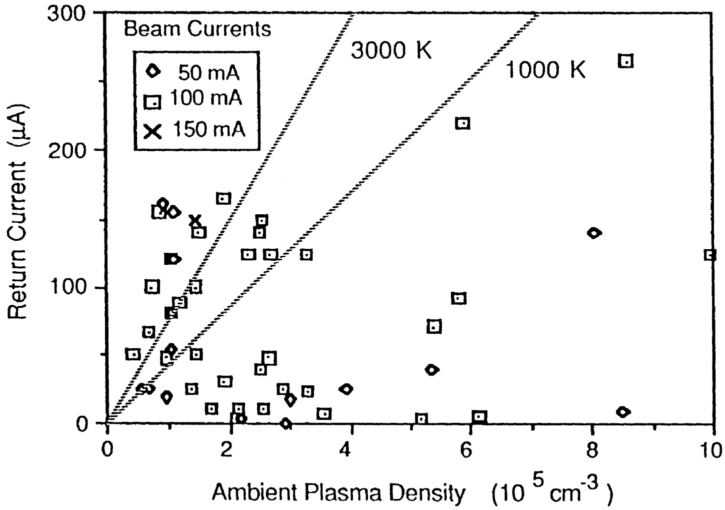

Fig. 2. Return current during DC electron beam emissions measured by the CCP current probe as function of ambient density estimated from the IRI model. As a reference is shown the ambient electron thermal current that can be drawn by the probe for two electron temperatures.

probe and $\boldsymbol{B}$ the earth's magnetic field. The potential shift is generally less than 5 V, which is enough to influence the electron current to the probe. The ion current is less affected since the ion energies seen from the reference frame of the Orbiter have energies larger than 5 eV (RAITT *et al.*, 1984).

In order to remove the obvious attitude bias in the Current Probe results, an Orbiter attitude called the airplane mode was selected. In this mode, the Shuttle orbits in the same manner as an airplane flies, and the wake structure around the Orbiter is constant. Furthermore, in this mode the $(\boldsymbol{V}_s \times \boldsymbol{B}) \cdot \boldsymbol{L}$ induced potential is always small. The result of selecting data from observations during the airplane mode is shown in Fig. 3. The probe current increases with ambient plasma density in a roughly linear fashion and seems independent of the emitted beam current. This trend in the data is important since it indicates that the beam does not fully escape the Orbiter. Rather it appears that the fraction of the beam that escapes is proportional to the ambient plasma density (the subset of CP data for the airplane mode all happen to be for low ambient plasma densities and high charging levels).

2.2 *Wave fields*

During the course of the 6 hour period when the PDP was free-flying, care was taken to permit the PDP and the Shuttle to have two magnetic conjunctions per orbit. The trajectory of the PDP relative to the Orbiter during the fourth conjunction is shown on the top panel of Fig. 4, with tick marks for every one minute of flight. The vertical axis is the distance to the PDP measured along the earth's magnetic field, and the horizontal axis the distance perpendicular to the field. A pulsed electron beam sequence was started at approximately 04:11 UT and lasted for about 7 min. The beam current was 100 mA and the beam was square-wave

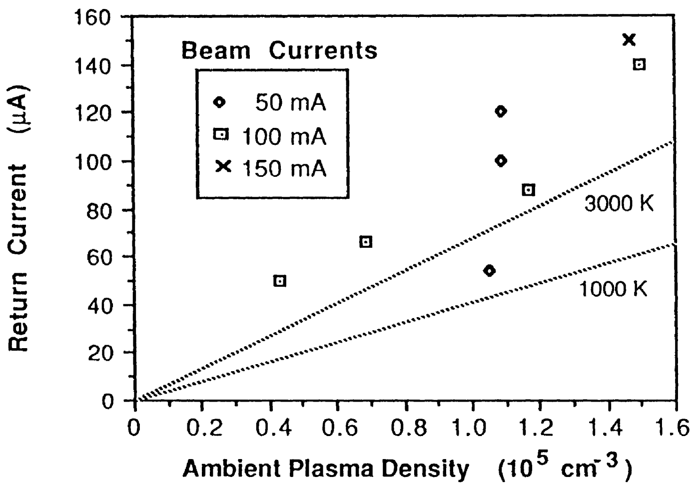

Fig. 3. Return current during DC electron beam emissions for a selected Orbiter attitude, the airplane mode.

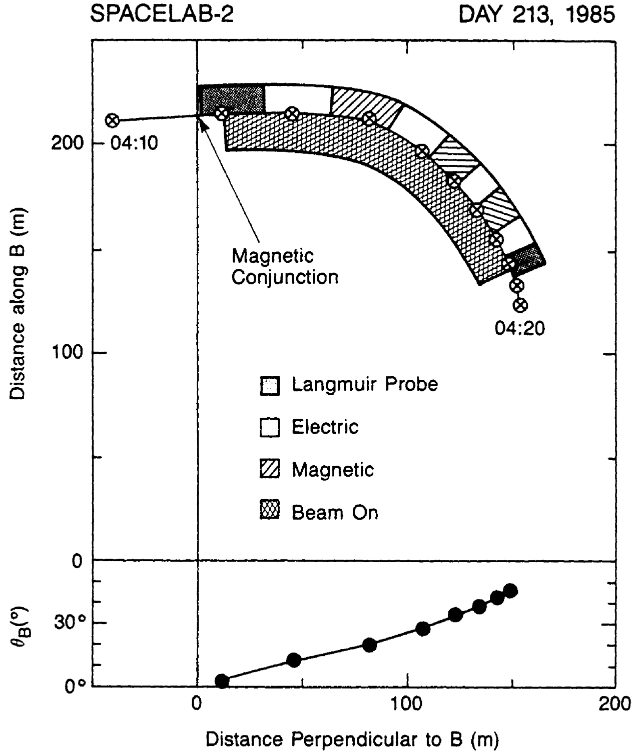

Fig. 4. On the top panel is shown the trajectory of the PDP relative to the Shuttle during the pulsed flux-tube connection. The period of beam emission and the wide band antenna switching pattern are shown by shaded areas. The bottom panel shows the beam angle θ_B with respect to the earth's magnetic field.

modulated at 1.22 kHz with a 50% duty cycle (beam on time equals beam off time). The period of beam emission and the antenna switching pattern of the wide-band wave receiver is indicated by shaded areas.

The Orbiter attitude was adjusted during this sequence so that the initial velocity of the beam electrons was always directed towards the PDP. The variation of the beam pitch angle is shown on the bottom panel of Fig. 4.

The conjunction occurred during nighttime. The ambient plasma density, estimated from the measurements of the Langmuir probe on the PDP, was 3.2×10^4 cm^{-3} (D'Angelo, personal communication), corresponding to a plasma frequency of 1.6 MHz, and the electron gyrofrequency varied from 560 kHz to 600 kHz. Assuming the ambient ion population consisted mainly of O^+, the lower hybrid frequency varied from about 3.1 kHz to 3.3 kHz.

An example of the magnetic field observed by the search coil on the PDP is shown in Fig. 5. The relative signal intensity (the AGC is not incorporated here) is color coded showing the fundamental and odd harmonics of the 1.22 kHz modulation frequency as horizontal lines. The first half of the panel, 0–25 s, the bandwidth is 0–10 kHz, the following quarter of the panel, 25–38 s, the band is 20–10 kHz, with 20 kHz being at the bottom of the frequency scale and 10 kHz at the top. The final quarter of the panel presents 20–30 kHz. During the time interval shown on Fig. 5 the perpendicular distance to the beam was about 75 m.

For comparison, Fig. 6 shows the electric field intensity observed 51.2 s earlier when the PDP was at a distance of about 40 m from the beam. As before, emissions are seen at the odd harmonics of the modulation frequency in the whole band. However, in addition to these coherent emissions, strong broad-banded electrostatic noise is also seen. This noise is about 40 dB above the background noise level observed prior to the beam emission and partly inhibits the detection of higher harmonics in the 0–10 kHz band.

The amplitude of the harmonics of the beam pulsing frequency have been estimated using a pre-flight calibration of the wide-band receiver and the AGC. The result of this calibration for the 0–10 kHz range is shown in Fig. 7 for the three time intervals during the pulsed beam emission that the receiver was connected to the magnetic search coil.

The Fourier transform of a square-wave function with a 50% duty cycle has vanishing even harmonics and possesses odd harmonics with amplitudes that vary with frequency as $1/f$. We note that the observed magnetic wave field does have strong odd harmonic components while the even harmonics, although present, are almost an order of magnitude weaker. This leads us to believe that the beam source, at least within the first couple of hundred meters, is able to retain much of its square-wave modulated structure (coherence in $v_{\|}$), in spite of the low ambient plasma density.

The electric field amplitudes are shown in Fig. 8. At larger distances from the beam, the second and third harmonic become relatively strong, while the first harmonic is strongly damped. This effect may be caused by the change in topology of the wave refractive index, which changes at the lower hybrid frequency (3 kHz for the experiment).

During its free-flight, the PDP was spinning with a period of 13 s. Both the magnetic and the electric sensors measured a component of the wave field perpendicular to the spin axis. This induces a modulation of the measured field amplitudes with a period of 6.5 s. The modulation is very noticeable in the magnetic field at all harmonic numbers and in the electric field for the harmonics with frequencies larger than 10 kHz. We expect an analysis of the amplitude modulation to give us important clues as to the polarization of the fields, and a means to check existing theories for wave generation by pulsed electron beams.

3. Discussion

Recent numerical simulations (WINGLEE and PRITCHETT, 1988) show that an electron beam will be strongly disrupted by the accumulation of negative space

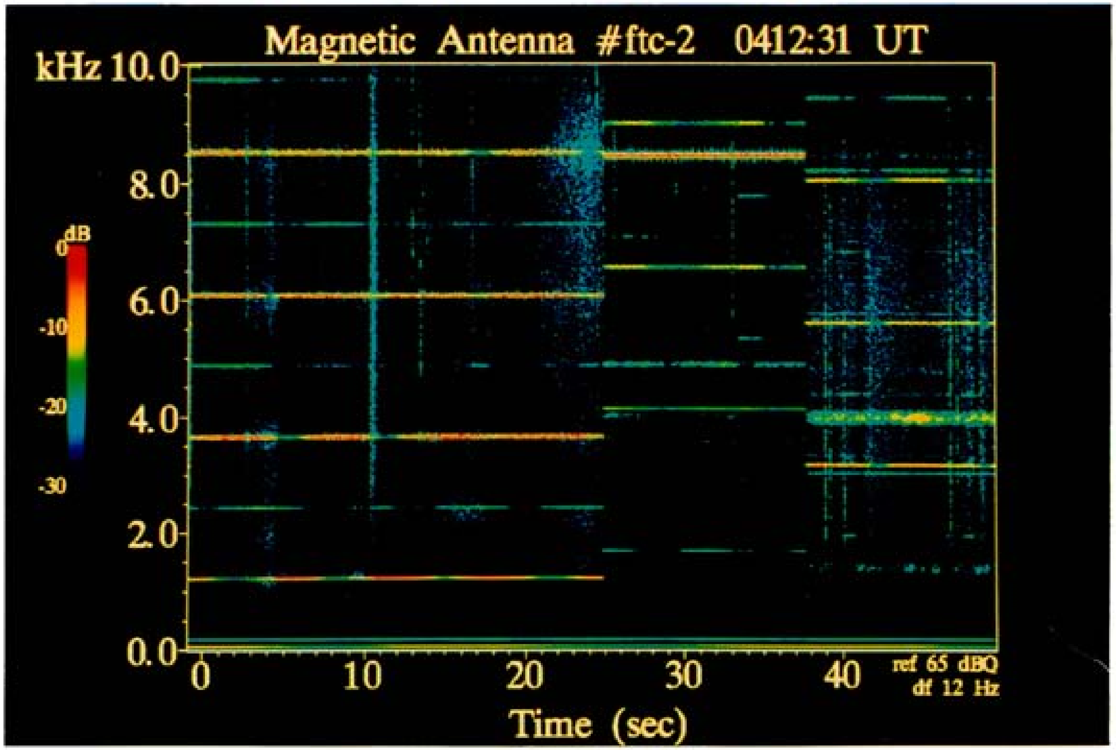

Fig. 5. The magnetic field in the frequency range 0–10 kHz, 20–10 kHz, and 20–30 kHz (see text) as a function of time. The perpendicular distance from the beam was about 75 m.

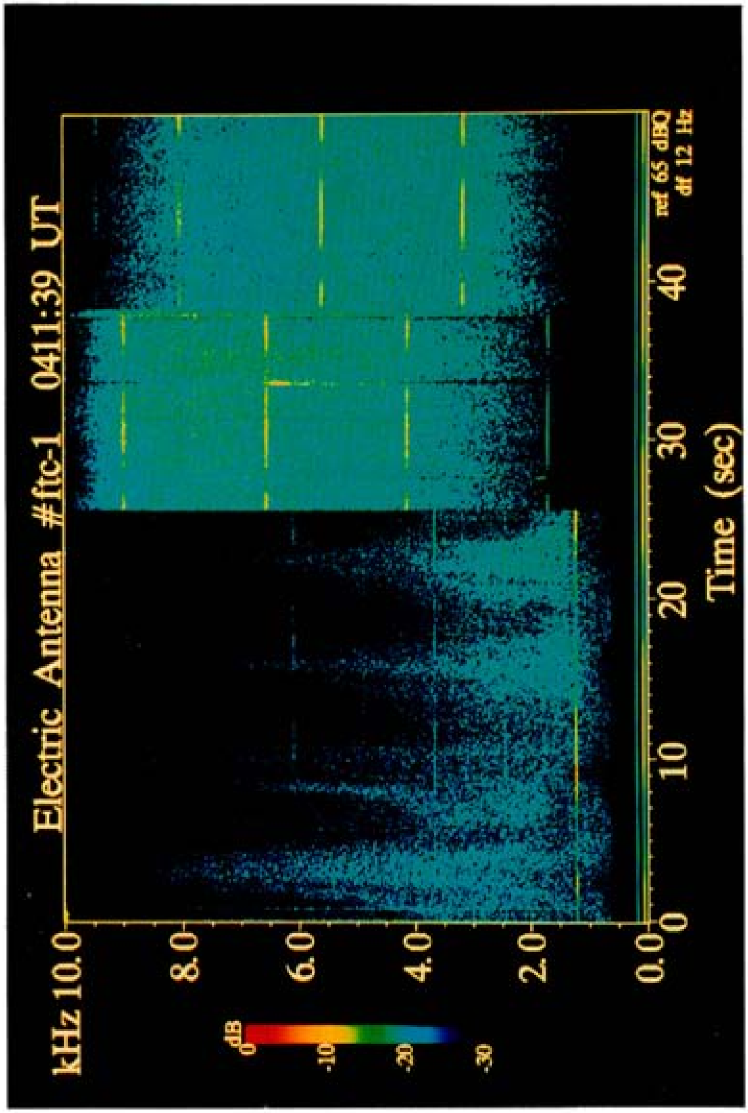

Fig. 6. The electric field the frequency range 0–10 kHz, 20–10 kHz, and 20–30 kHz (see text) as function of time. The perpendicular distance to the beam was about 40 m.

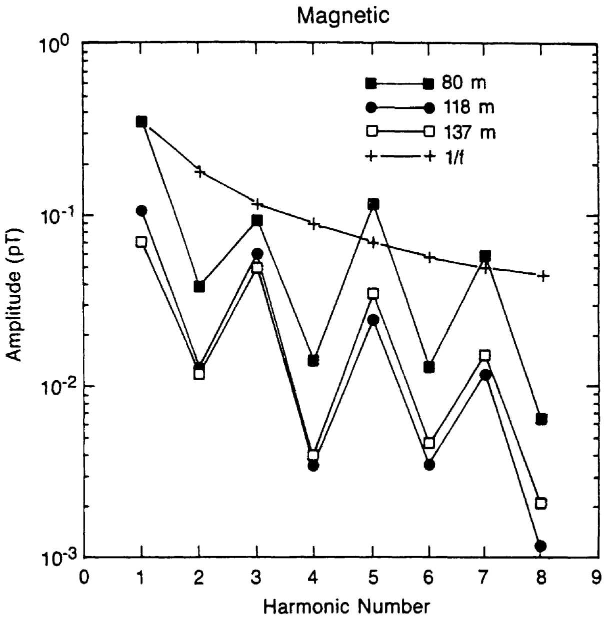

Fig. 7. Amplitude of the harmonics of the beam pulsing frequency (magnetic) at three radial distances from the beam. Also shown for reference is a $1/f$-functional dependance, where f is frequency (or harmonic number)

charge in a region close to the beam nozzle if the beam density at injection is much larger than the ambient ionospheric density. The formation of such a virtual cathode is found to develop if $t_{rp}/t_s > 0.4$, where t_{rp} is the plasma response time and t_s is the beam stagnation time. The plasma response time is about $\sqrt{3}/\omega_{pe}$, where ω_{pe} is the electron plasma frequency of the ambient ionosphere. The beam stagnation time depends on the spacecraft size, the beam width and the beam energy and is for Spacelab-2 conditions in the range $5/\omega_{pb}$ to $15/\omega_{pb}$, where ω_{pb} is the beam plasma frequency at beam injection. The FPEG beam density at injection has been estimated to be about 3×10^7 cm^{-3} (BANKS and RAITT, 1988) and the ambient plasma density during the pulsed flux tube connection was about 3.2×10^4 cm^{-3} as measured by a Langmuir probe mounted on the PDP. Thus for the experimental conditions we have $\omega_{pb}/\omega_{pe} = 30.6$, or $t_{rp}/t_s = 3.5$ to 10.6. These values are much larger than the threshold value of 0.4, and according to the computer simulations we should expect strong beam disruption and limitations in the amount of beam current escaping the Orbiter.

The Current Probe measurements shown in Fig. 3 seem to be in accordance with the predictions of WINGLEE and PRITCHETT (1988). At low ambient plasma densities, the fraction of the beam that escapes the Orbiter increases with the ambient density. The voltage measured by the Charge Probe during the pulsed flux-tube connection was about 40 V, a value in accordance with the results shown

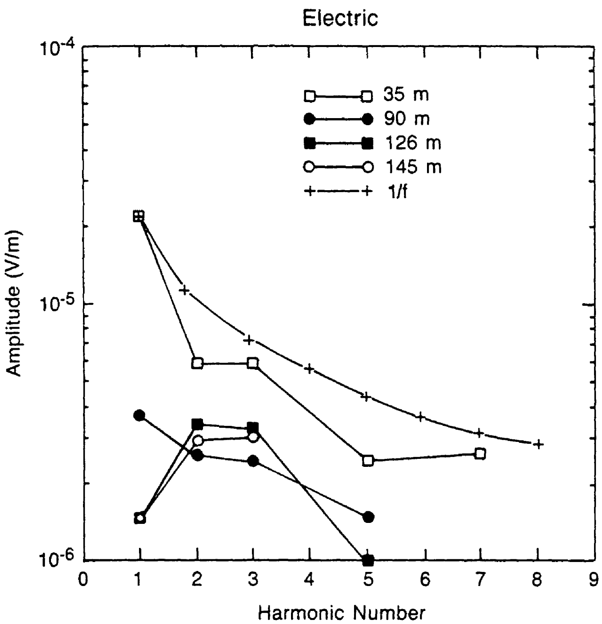

Fig. 8. Amplitude of the harmonics of the beam pulsing frequency (electric) at four radial distances from the beam.

in Fig. 1 for 50 mA beams (100 mA, 50% duty cycle). The Orbiter is charging to a relatively high potential, because the ambient plasma density of 3.2×10^4 cm^{-3} is lower than the threshold value of 1.5×10^5 cm^{-3} for 50 mA beams. As mentioned earlier, the Orbiter potential may have been higher than indicated by the Charge Probe.

However, we are reluctant to draw any firm conclusions on beam escape on the basis of the limited dataset presented in Fig. 3. The return current distribution is probably strongly non-uniform and sensitive to small changes in the attitude and magnetic field variations. Furthermore, the wave data indicate that the beam retains its coherent structure during the pulsed flux-tube connection, with at least a portion of the beam fully escaping the Orbiter.

REEVES *et al.* (1988b) noted that the intensity and spectral shape of the broad-banded, mainly electrostatic, noise observed both at low frequencies by the wide-band receiver and at high frequencies by the filterbank, was almost the same during a DC flux-tube connection, performed earlier during the PDP fly-around (GURNETT *et al.*, 1986), and the pulsed flux-tube connection. The effective current was the same for the two sequences, 100 mA pulsed with 50% duty cycle and 50 mA DC. However, while the two beam experiments were performed with the PDP at similar locations relative to the Orbiter and the beam, the ambient plasma density was higher during the DC flux-tube connection. The value for the density was about 10^5

cm^{-3}, which gives $t_{rp}/t_s=2$ to 6. These values are again above the threshold of 0.4. The potential measured by the Charge Probe was about 3 V or less.

With the Orbiter charging to high levels during the pulsed sequence, and low levels during the DC sequence, the similarity of the broad banded wave emissions indicate that either the two beams were both strongly disrupted, or both escaped the Orbiter largely unaffected by space charge effects.

The magnetic component of the coherent signals generated by the pulsed beam has strong odd harmonic components as compared to the even harmonic components, with the amplitude of the odd harmonics roughly varying like $1/f$ (see Fig. 7). This indicates that the source is basically square-wave modulated with little distortion in the parallel electron beam velocity. Thus we are lead to conclude from the wave data that the beams escaped the Orbiter largely unaffected by space charge effects.

The question of the fraction of the beam current that, in given circumstances, can escape a space platform is fascinating, but experimentally very hard to solve. Our experience from the Spacelab-2 experiment indicates that wave measurements may prove to be a powerful tool to answer this question once the generation process is thoroughly understood. However, at present the details are still debated.

It was found that the high frequency wave intensity observed by the filterbank during the DC and pulsed flux-tube connections had a funnel like appearance in frequency/time spectrograms and that this feature was consistent with whistler waves generated through a Landau resonance with beam electrons in a semi infinite beam (GURNETT *et al.*, 1986; REEVES *et al.*, 1988b). The radiation level is in accordance with the level predicted by quasi coherent Cherenkov resonance provided the beam electrons have a coherence length of about 7 m (FARRELL *et al.*, 1988). The radiation level of Cherenkov resonance depends strongly on the beam coherence length, which in FARRELL *et al.* (1988) was assumed to be determined by the wavelength of Langmuir oscillations generated inside the beam column.

However, recent numerical results of simulations of the Spacelab-2 DC beam (OMURA and MATSUMOTO, 1988) indicate that funnel shaped emissions may be generated even by infinite beams. In their simulations the funnel is due to frequency dependent damping of the waves as they propagate away from the beam. Furthermore, they found that the wave length of the electrostatic wave noise generated inside the beam column does not match the wave length of the radiated whistler mode noise and concluded that the radiation was not caused by bunching of beam electrons as proposed by FARRELL *et al.* (1988).

With a thorough understanding of the radiation process through which wave emissions are produced by DC and pulsed electron and ion beams, wave measurements may in the future be used as quantitative remote diagnostic tools to probe artificial and natural beam structures in space.

One of the authors (T. Neubert) thanks Kyoto University for travel support to the Kyoto WACTEXS meeting. The work done at Stanford was sponsored by NASA under contracts NAGW-235 and NAG5-476. NASA's Space Physics Analysis Network (SPAN) was used in

the preparation of this report.

REFERENCES

BANKS, P. M. and W. J. RAITT, Observations of electron beam structure in space experiments, *J. Geophys. Res.*, **93**, 5811–5822, 1988.

BANKS, P. M., W. J. RAITT, A. B. WHITE, R. I. BUSH, and P. R. WILLIAMSON, Results from the vehicle charging and potential experiment on STS-3, *J. Spacecraft*, **24**, 138–149, 1987.

BILITZA, D., International reference ionosphere: Recent developments, *Radio Science*, **21**, 343–346, 1986.

BUSH, R. I., G. D. REEVES, P. M. BANKS, T. NEUBERT, P. R. WILLIAMSON, W. J. RAITT, and D. A. GURNETT, Electromagnetic fields from pulsed electron beam experiments in space: Spacelab-2 results, *Geophys. Res. Lett.*, **14**, 1015–1018,1987.

FARRELL, W. M., D. A. GURNETT, P. M. BANKS, R. I. BUSH, and W. J. RAITT, An analysis of whistler mode radiation from the Spacelab-2 experiment, *J. Geophys. Res.*, **93**, 153–161, 1988.

GREBOWSKY, J. M., H. A. TAYLOR, and M. W. PHARO, Thermal ion perturbations observed in the vicinity of the space shuttle, *Planet. Space Sci.*, **35**, 501–513, 1987.

GURNETT, D. A., W. S. KURTH, J. T. STEINBERG, P. M. BANKS, R. I. BUSH, and W. J. RAITT, Whistler-mode radiation from the Spacelab-2 electron beam, *Geophys. Res. Lett.*, **13**, 225–228, 1986.

HAWKINS, J. G., Charging and return current measurements during electron beam experiments from the shuttle orbiter, Thesis, Stanford, 1988.

HOLZWORTH, R. H. and H. C. KOONS, VLF emissions from a modulated electron beam in the auroral ionosphere, *J. Geophys. Res.*, **86**, 853–856, 1981.

OMURA, Y. and H. MATSUMOTO, Computer experiments on whistler and plasma wave emissions for Spacelab-2 electron beam, *Geophys. Res. Lett.*, **15**, 319–322, 1988.

PRITCHETT, P. L. and R. M. WINGLEE, The plasma environment during particle beam injection into space plasmas, 1, Electron beams, *J. Geophys. Res.*, **92**, 7637–7688, 1987.

RAITT, W. J., D. E. SISKIND, P. M. BANKS, and P. R. WILLIAMSON, Measurements of the thermal plasma environment of the space shuttle, *Planet. Space Sci.*, **32**, 457–467, 1984.

REEVES, G. D., P. M. BANKS, A. C. FRASER-SMITH, T. NEUBERT, R. I. BUSH, D. A. GURNETT, and W. J. RAITT, VLF wave stimulation by pulsed electron beam injected from the space shuttle, *J. Geophys. Res.*, **93**, 162–174, 1988a.

REEVES, G. D., P. M. BANKS, T. NEUBERT, R. I. BUSH, P. R. WILLIAMSON, A. C. FRASER-SMITH, D. A. GURNETT, and W. J. RAITT, VLF wave emissions by pulsed and DC electron beams in space I: Spacelab-2 results, submitted to *J. Geophys. Res.*, 1988b.

SASAKI, S., N. KAWASHIMA, K. KUKURI, M. YANAGISAWA, and T. OBAYASHI, Vehicle charging observed in SEPAC Spacelab-1 experiment, *J. Spacecraft*, **23**, 194–199, 1986.

SHAWHAN, S. D., G. B. MURPHY, P. M. BANKS, P. R. WILLIAMSON, and W. J. RAITT, Wave emissions from dc and modulated electron beams on STS-3, *Radio Science*, **19**, 471–486, 1984.

SISKIND, D. E., W. J. RAITT, P. M. BANKS, and P. R. WILLIAMSON, Interaction of the orbiting space shuttle and the ionosphere, *Planet. Space Sci.*, **32**, 881–896, 1983.

WATERMANN, J., K. WILHELM, K. M. TORKAR, and W. RIEDLER, Space shuttle charging or beam-plasma discharge: What can electron spectrometer observations contribute to solving the question?, *J. Geophys. Res.*, **93**, 4134–4140, 1988.

WINCKLER, J. R., K. N. ERICSON, Y. ABE, J. E. STEFFEN, and P. R. MALCOLM, ELF wave production by an electron beam emitting rocket system and its suppression on auroral field lines: evidence for Alfven and drift waves, *Geophys. Res. Lett.*, **12**, 457–460, 1985.

WINGLEE, R. M. and P. L. PRITCHETT, Comparative study of cross-field and field-aligned electron beams in active experiments, *J. Geophys. Res.*, **93**, 5823–5844, 1988.